Noise Transmission through a Glass Window excited by Low-Speed Turbulent Flow

Rémi Bessis, Yves Gervais, Laurent-Emmanuel Brizzi, Janick Laumonier

ACOUSTICS 2012

Noise Transmission through a Glass Window excited by Low-Speed Turbulent Flow

R. Bessis, Y. Gervais, L.-E. Brizzi and J. Laumonier

Institut Pprime, CNRS - Université de Poitiers - ENSMA, ENSIP, 6 rue Marcel Doré, Batiment B17, BP 633, 86022 Poitiers, France
remi.bessis@univ-poitiers.fr

In order to improve on-board automotive acoustic comfort, we investigate the effects of vortex dynamics and unsteady flow separation outside the lateral window of a car on the inside noise radiation through the window. Different mechanisms are expected to contribute to the transmitted aerodynamic noise. One is related to the acoustic excitation in the environment of the window and a second mechanism is influenced by direct hydrodynamic excitation of the window. Experiments have been performed in an open low-speed wind tunnel including a forward-facing-step geometry in order to generate vortex shedding above a window. An anechoic cavity under the glass allows the detection of the transmitted sound. Surface-pressure fluctuations and outside velocities (PIV) were estimated simultaneously. Spectral density and correlation-based signal processing were implemented to link flow structures to acoustic transmission. Proposals for separation of the contributions behind noise transmission involving variations of timescales and lengthscales on the flow are also presented.

Introduction

The A-pillar, the corner edge between the windshield and the front side window, is among the most critical aerodynamic components of an automobile [1]. The flow by-passing the A-pillar generates an intense three-dimensional coherent structure (the A-pillar vortex) which is a source of surface pressure fluctuations on the front side window as well as a source of aerodynamic noise, resulting from the transfer of a part of kinetic energy of the turbulent volumetric flow structures into acoustic energy, interacting with the window. Direct vorticity excitation of the window, which we designate as hydrodynamic, is associated with the spreading of turbulent structures above the window. This highly energetic excitation mainly contributes to the low frequencies whereas acoustic excitation is predominant into the mid and high frequency domains, where spatially coherent acoustic waves matches with the vibrations of the window. This is a major concern in the vicinity of the acoustic coincidence frequency of the window.

A key step in understanding the mechanisms involved in sound transmission inside a vehicle is the separation of hydrodynamic and acoustic contributions to the inner acoustic field. This is a complicated task in the present case because the problem mixes a turbulent flow with highly non-uniform characteristics and a complex vibro-acoustic problem, the vibrations of the window. Technics commonly used are schematically twofold. The first one implements spatio-temporal analysis with two-dimensional wavenumber-frequency domain filtering methods. This has been used with mixed success but is still commonly applied to surface pressure analysis. It is usually based on a Corcos or Chase model [2][3] and it has for instance been applied to two-dimensional geometries and even A-pillars [4][5][6]. The second strategy, that we chose, is based on correlation technics in signal processing. Previous studies investigate the hydrodynamic mechanisms on wall-pressure fluctuations with geometries such as a disk located in the vicinity of a flat wall [7], various step geometries [12] or a "MOPET body" [8]. However, very few include considerations on both the wall pressure and the acoustic field. Among those, D. Leclerc [9] investigated the mechanisms of sound transmission through a thin flat metal-plate under turbulent boundary layer excitation.

Within the present study, we consider a turbulent separated flow formed along the edge of forward facing-step geometry. This geometry was selected because of two simplifying features. First, the flow passing this two-dimensional geometry has a practical advantage over A-pillar vortex type flow as measurements are two-dimensional. Then, previous investigations carried-out on this specific (or similar) geometry provide comparative data against which the methods can be tested. In the following, the structure of this typical flow is briefly described. Measurements which demonstrate the flow structure (including considerations on the velocity field and the surface-pressure fluctuations) are presented as preliminary verifications to later coherence-based aeroacoustic analysis (wall-pressure and acoustic field).

1 Experimental procedure

1.1 EOLE (anechoic wind-tunnel)

Experiments were conducted in the anechoic sub-sonic Eiffel-type wind-tunnel EOLE of the P' institute (Poitiers, France). The flow enters a $(4\times3\times3)m^3$ anechoic chamber through a $(46\times46)cm^2$ convergent nozzle and is sucked through a $(1.2\times0.8)m^2$ collector. Side walls are used to connect the convergent nozzle to the collector in order to improve the two-dimensionality of the flow between the walls [12], so the measurement area is ¼ open. Between the side-walls a removable flat plate emerges from under the flow and creates a two-dimensional forward facing-step geometry with 30mm height. The plate is either a rigid instrumented flat plate used for wall-pressure measurements or a rigid flat plate with a thin rectangular $(46\times20)cm^2$ window capable of vibrating under a turbulent load. For the latter configuration, a box is located directly under the step to allow measurements of the noise transmitted through the window. The cavity has an internal volume of approximately $0.35m^3$ and consolidation on the external surface area which ensures sufficient sound insulation regarding background noise in the chamber. The inside cavity has an anechoic treatment. The structure is illustrated in Fig.1. Test speeds for the wind, denoted as U_{inf}, ranges from 30 to 50 m s^{-1} (110 to 180 km h^{-1}).

1.2 Instrumentation

For all tests, velocities in the flow were estimated simultaneously to wall pressure or acoustic field. For the surface pressure measurements, differential remote probes were used. Frequency cutoff for the actual system is approximately 1.3kHz and pressure range is 1250 Pa. To take into account the effects of the tabbing system (delays, resonance modes, etc), Frequency Response Functions were used to correct the magnitude and the phase of the resulting spectra. Preliminary surface flow visualizations were performed in order to help to determine the optimal positions for the surface pressure measurements. Positions for the time-mean reattachment lines were estimated and the front part of the step was instrumented with a total of 63 small inserts (1.3mm diameter) arranged as follows: 31

inserts in the direction of the model centerline (L_1), 2×16 inserts in the transversal direction, upstream (L_2) and downstream (L_3) the mean-reattachment lines. Minimum spacing between two inserts is 5mm. 16 probes were used behind the inserts for simultaneous acquisitions. Measurements in the direction of the flow give access to the fluctuations in relation to the flow intermittencies whereas transversal measurements were mainly used to discuss the two-dimensionality of the flow. The amplified signals from the sensors have been recorded at a sampling frequency 6250Hz by a multi-channel acquisition system ETEP.

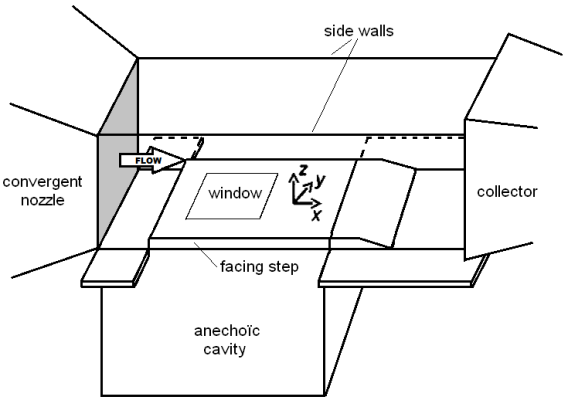

Figure 1. Experimental set-up (acoustic measurements). Origin for the Cartesian coordinates is located at the edge of the step, at the centre of the test section.

The velocity fields were obtained with two components Particle Image Velocimetry (PIV). Both the longitudinal and the vertical velocity components were measured. Illumination was provided by a double pulsed Nd:YAG laser and raw PIV images were acquired at a frequency rate of 5 Hz with a LaVision camera counting (1376×1040)pixels^2. The velocity fields were then computed via Davis 7.2 software implementing a multipass algorithm with a final interrogation window size of (16×16) pixels^2 and a 50% overlap. Velocities were estimated in near wall planes with the center of the image around the time-mean reattachment line in the flow, at 2 mm and 5 mm from the surface area, and in a symmetry plane in the direction of the model centreline (Fig.2).

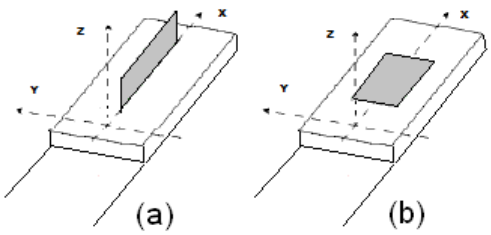

Figure 2. PIV set-up : (a) symmetry plane ; (b) planes parallel to the surface of the step (2mm & 5mm)

Lastly, the far field acoustic pressure inside the chamber (the outside acoustic field) and the noise inside of the cavity, transmitted through the window (inner noise), were estimated using ½–inch condenser microphones from Brüel&Kjaer. Outside measurements implemented three microphones, regularly arranged to cover the distance from the convergent nozzle to the collector and two microphones were used inside the cavity. All microphones were connected to a conditioning amplifier and signals were recorded at a sampling frequency of 25kHz by the multi-channel acquisition system ETEP, which gives a 10kHz frequency bandwidth.

2 Outside flow characterization: flow over forward facing step

2.1 Time-mean structure of the flow

The time-mean structure of the unsteady separated and reattaching turbulent flow over forward facing-step is illustrated on Fig.3. The flow is central to many studies and the present document does not intend to review the current state of knowledge of forward facing-step flow. For more insight into the topology of this typical flow, one should refer to comprehensive investigations [10]&[11]. More recently, Largeau [12] investigated the flow over a forward facing-step with similar experimental conditions to the ones that we use (R_{eh}, U_{inf}, turbulence rate,…). Investigations were made in terms of velocity and wall pressure measurements, as we do. Valuable information obtained by Largeau was used as a comparison to test the methods here.

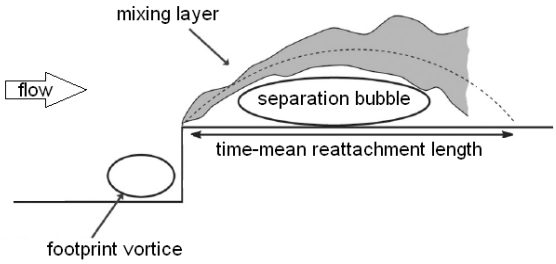

Figure 3. Mean structure of flow over forward facing-step geometry.

2.2 Statistic results

In order to improve physical understanding of the phenomena involved in the excitation of the window, time-mean analysis was performed on velocity and surface pressure measurements with special attention to lateral homogeneity in the flow. Fig.4 shows calculations of the time-average velocity norm in the symmetry and near-wall planes. One thousand statistically PIV uncorrelated velocity fields were necessary to obtain converged statistics. Only the results for U_{inf}=30 ms^{-1} are presented, but whatever the speed of the flow in the test speed range, statistics in the planes parallel to the surface of the step are in fairly good agreement with the assumption of homogeneity in the flow for the lateral direction. In the plane of the measurements, results show no effects from the side walls along the test section. Analysis of the distribution of pressure fluctuations over the surface of the step confirms the latter. Fig.5 presents the variation of the root-mean-square coefficient of pressure fluctuation, $C_{p'}$, along the centerline L_1 and lines L_2 and L_3, and it is obvious here that pressure fluctuations are uniformly distributed along the lateral direction. The expression used for the coefficient calculation is given in

Eq.(1), where $<p^2>$ is the variance and p the fluctuating pressure:

$$C_{p'} = \sqrt{\langle p^2 \rangle} / (\rho U_{inf}/2) \quad (1)$$

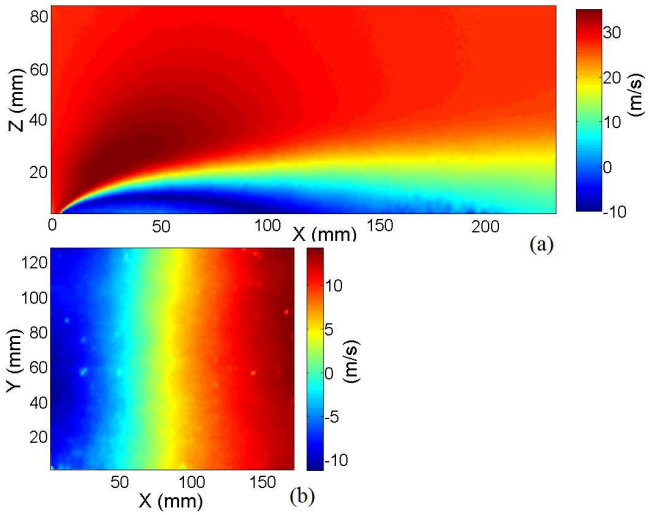

Figure 4. Time-mean norm velocity with U_{inf}=30m/s in: (a) the symmetry plane; (b) the parallel plane (at 2mm).

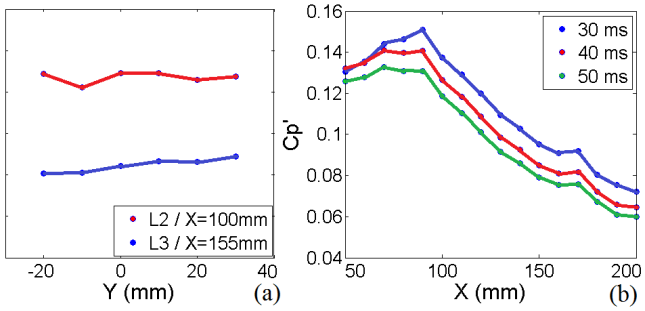

Figure 5. Coefficients $C_{p'}$: (a) L_2 and L_3 with U_{inf}=30m/s; (b) along L_1 for different flow speeds.

Taking into account previous the homogeneity of the flow, it seems reasonable to consider mean-results based on the measurements in the plane of symmetry (pressure and velocity) as representative for the structure of the flow in the lateral direction. Velocity statistics in the plane of symmetry (Fig.4(a)) demonstrate the structure of a turbulent separation bubble, formed along the front of the step (X=0 mm), with the typical acceleration of the flow on the top part of the shear layer, which progressively transforms into turbulent boundary layer downstream from the mean-reattachment point (X=L_R). The dimensions of the bubble are consistent with the measurements made by Largeau. In particular, the positions L_R, estimated for U_{inf}=30, 40 & 50ms^{-1} to 130, 120 &110mm respectively, are in good agreement with the lengths measured by Largeau (L_R≈90-150mm). It has also been ensured that the length of the separation bubble decreases with an augmentation of the external flow speed. Repartition of the $C_{p'}$ along the model centerline L_1 is coherent with PIV measurements as one can clearly notice that maximum level for the fluctuations is reached slightly upstream of reattachment point X/L_R=1, followed by a strong decrease in the coefficient downstream this position: the trend, common to all the speed regimes, is in fairly good agreement with the investigations from Kiya & Sasaki [10], who report a maximum of pressure fluctuations located upstream the mean-reattachment line, near position X/L_R=0.9.

3 Spectral density and coherence analysis for surface fluctuating pressure and acoustic under the turbulent flow

3.1 Post-processing

Auto-power spectral densities and coherences calculations were applied both to acoustic measurements than wall-pressure fluctuations as an attempt to estimate the timescales of the acoustic noise sources and hydrodynamic fluctuations in the flow, respectively. Coherence-based analysis is used in order to remove statistically incoherent noise in the measurements. The method involves the calculation of the coherence function γ^2. The ordinary formulation for the coherent function was defined by Bendat and Piersol [13] for two sensors (denoted i and j), as

$$\gamma_{i,j}^2(\omega) = |G_{i,j}(\omega)|^2 / [G_{i,i}(\omega) G_{j,j}(\omega)] \quad (2)$$

where $G_{i,i}$ and $G_{j,j}$ are the auto-spectrums and $G_{i,j}$ the cross-spectra between signals i and j. Power spectrum calculations implement the classic one-sided fast Fourier transform of the discrete signals. We use 1024-point Fourier transforms and a minimum of 2500 mean results are included in the calculation.

3.2 Analysis of wall pressure fluctuations

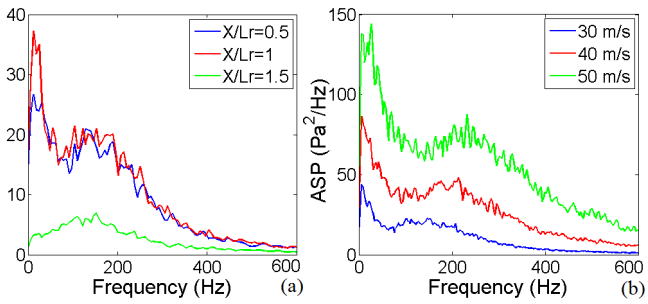

Figure 6. Auto power spectral (ASP) densities of wall pressure fluctuations: (a) at different positions along the model centre line (U_{inf}=30m/s); (b) position X/L_R=1 with changing flow speed.

The surface pressure spectral densities measured at various positions are given for U_{inf}=30m/s on Fig.6(a). The energy in the signals is essentially concentrated at low frequencies (bellow 500Hz) where hydrodynamic phenomena occur. Analysis of the spectra reveals the next characteristics for the flow. In the vicinity of the reattachment point (X/L_R=1), higher levels for the surface pressure are around 20Hz and 150Hz. Observations on the spectral densities in the very first frequencies (below 100Hz) should be considered with care, as in this frequency domain the contributions can interfere with the important

background noise in the chamber, inherent in the wind tunnel EOLE. Here, coherence calculations between two sensors in the vicinity of this position (positions X/L_R =0.92 and 1.08 on Fig.7) are very handy and highlight more precisely the maxima in the spectrum, for 20Hz as well as for 150Hz. According to Kiya &Sasaki [10], these specific frequencies correspond to Strouhal numbers (based on the time-mean reattachment length) of 0.12 and 0.6 and are related to the flapping motion of the separation bubble and the unsteady shedding of vorticity from the bubble. Spectral densities and coherence repartition along the model centreline are in very good agreement with previous statements as both the flapping and shedding frequencies are present in the vicinity and upstream of position $X=L_R$. Downstream the reattachment point, the shedding frequency remains, whereas the flapping motion is no more detected, neither on the spectral densities nor on the coherence calculations. With an increase in the wind speed (Fig.6(b)), maxima in power densities are shifted to higher frequencies, which demonstrate once again the hydrodynamic nature of the phenomena involved. Measurements lead to slightly lower (but still acceptable) averaged Strouhal numbers of 0.09 for the flapping and of 0.55 for the shedding.

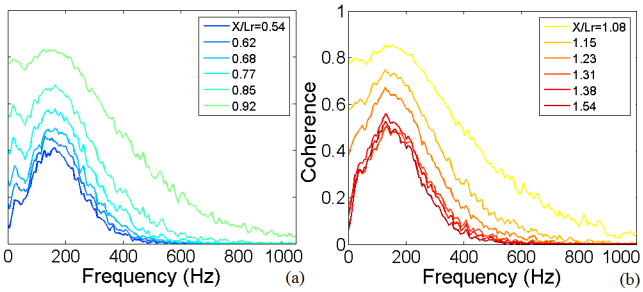

Figure 7. Coherence calculation results along L_1 (U_{inf}=30m/s), between the sensors near X/L_R=1 (reference) and: (a) the positions X/L_R<1; (b) the positions X/L_R>1.

3.3 Acoustic analysis

During the acoustic tests, three different plate-windows were used, which behave differently to the turbulent load. The windows mainly differ from each other in terms of their hydrodynamic and acoustic coincidence frequencies. These characteristics were used as filters in the frequency domain in order to highlight the mechanisms involved in the noise transmission through the window with particular attention to the contribution of the coincidences to the inner noise. Coincidences in the low frequency domain are related to vorticity above the window and so, depend on the external flow speed (U_{inf}) as well as on the mechanic characteristics of the material the window is made of. Coincidences in mid and high frequencies are acoustic by nature and occur when the propagation speed of the bending wave into the material equals or exceeds the speed of sound in the air, resulting in propagative waves into the window. The following notations are used in the following for the different windows used: W_1 for a 3mm thick plastic window, W_2 and W_3 for 2mm and 3mm thick glass windows, respectively.The theoretical frequencies are collected on Tab.1. Measurements on a reverberant chamber with an external diffuse sound field have been performed and the results obtained were virtually identical to the theory.

Window	Hydrodynamic	Acoustic
W1	120-350 Hz	15300 Hz
W2	50-130 Hz	5900 Hz
W3	30-90 Hz	3900 Hz

Table 1. Theoretical coincidences for the windows. Hydrodynamic frequencies are presented for U_{inf}=30m/s to 50m/s (the lower hydrodynamic frequency corresponds to the lower flow speed).

Auto power spectral densities and coherence calculations for inner microphones, are collected on Fig.8 and 9, respectively, for a flow speed U_{inf}=40m/s. Results were as expected. On the spectral densities, the window with a higher hydrodynamic coincidence (W_1) appeared to predominate in the low frequency domain (with an emergence of at least 15dB between 300Hz and 700Hz) whereas, in mid frequencies, high levels in the densities are reached in the vicinity of the coincidence frequencies, around 6000-7000Hz (W_2) and 3000-4000Hz (W_3). This trend is even more accentuated on the coherence results. In fact, coherence functions reach high levels in the vicinity of the acoustic coincidences for windows W_3 and especially W_2 (up to 50- 60% near coincidence).

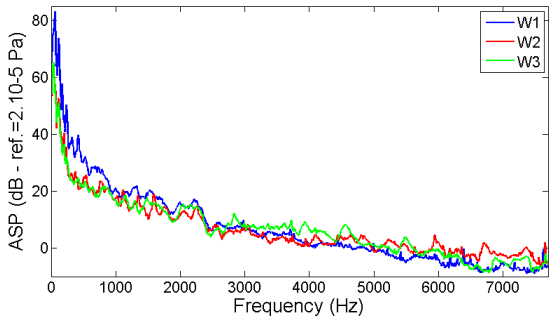

Figure 8. ASP densities for the inner acoustic field with U_{inf}=40m/s.

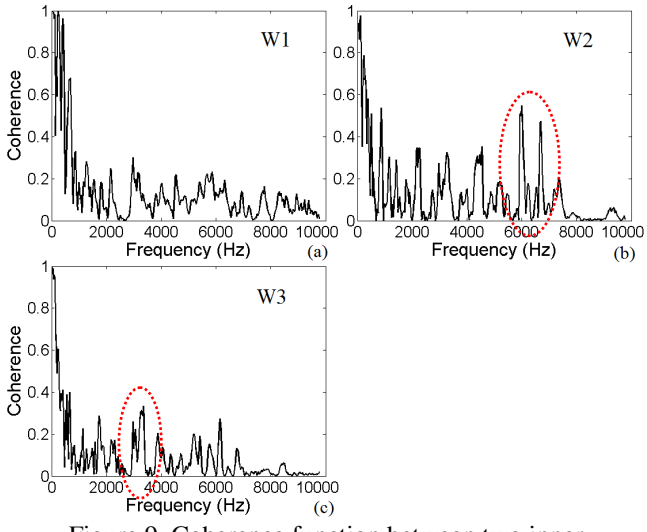

Figure 9. Coherence function between two inner microphones, with different windows (U_{inf}=40m/s).

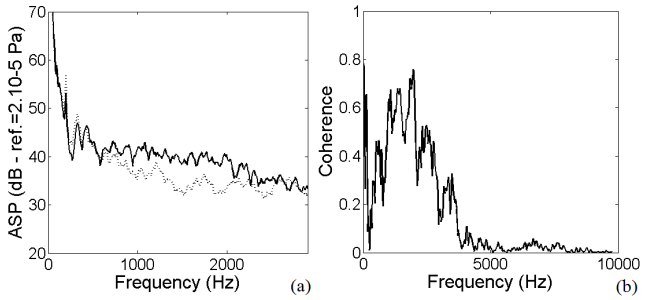

Figure 10. Acoustic in the chamber (U_{inf}=40m/s): (a) superposition of the ASP densities with the forward facing step and a turbulent boundary layer (dashed line); (b) outside coherence calculation with the step.

The chamber acoustic field has also been investigated. Power spectral density and coherence function between two microphones in the outside acoustic field are given on Fig.10. Both results demonstrate the wideband noise print for the outside acoustic field generated by the model used. Outside acoustic contribution for current forward facing step was estimated to [500Hz-3000Hz], what is in good agreement with the [400Hz-3800Hz] bandwidth measured by Largeau [12]. Whatever the velocity of the flow, outside measurements yielded very similar results. An interesting fact is the absence of coherent acoustic energy in the frequency domain where the acoustic coincidences occur, above 3000Hz. This is a very informative result as it could reveal "hidden" directive noise generation within the flow. In the mid frequency domain, coherent acoustic behind the window W_2 (and maybe W_3) may reasonably be considered as unrelated to the chamber's background noise but rather related to mid frequency acoustic excitation generated within the flow above the window.

4 Conclusion

The present study is a work in progress. Investigations on a forward facing step have been carried-out in terms of surface pressure fluctuations, velocities in the flow and acoustic transmission. Statistical analysis allowed us to successfully test the structure of the flow as well as the experimental procedure and the methods. Temporal analysis applied to wall pressure fluctuations added more insights into the hydrodynamic mechanisms acting within the flow. Finally, coherence-based analysis applied to both outside and inner acoustic fields highlight the acoustic transmission path in relation to the coincidences of the window. Vibration analysis for the windows should complement current data set in order to develop present analysis and define more precisely the mechanisms behind noise generation in the flow.

Acknowledgments

The authors warmly acknowledge Laurent Philippon, Pascal Biais and Pascal Braud for their technical support. The PhD of Rémi Bessis is co-financed by CNRS (France) and the CNRT "Aérodynamique et Aéroacoustique des véhicules terrestres".

References

[1] W.H. Hucho, "Aerodynamics of road vehicles: from fluid mechanics to vehicle engineering", SAE, ISBN (1998)

[2] G.M. Corcos, "Resolution of pressure in turbulence", *J. Acoust. Soc. Am.* **35**, 192-199 (1963)

[3] D.M. Chase, "The character of the turbulent wall pressure spectrum at subconvective wavenumbers and a suggested comprehensive model", *J. Sound and Vibration* **112**, 125-147 (1987)

[4] B. Arguillat, D. Ricot, C. Bailly, G. Robert, "Measured wavenumber : Frequency spectrum associated with acoustic and aerodynamic wall pressure fluctuations", *J. Acoust. Soc. Am.* **128**, 1647-1655 (2010)

[5] S. Debert, M. Pachebat, V. Valeau, Y. Gervais, "Ensemble-Empirical-Mode-Decomposition method for instantaneous spatial-multi-scale decomposition of wall-pressure fluctuations under a turbulent flow", *Exp. Fluids* **50**, 339-350 (2011)

[6] S. Vergne, F. Van Herpe, J. Viot, "Spatio-temporal analysis of wall pressure fluctuations on several automotive side-glasses", *International Journal of Aerodynamics* **1**(3-4), 354-372 (2011)

[7] T. Ruiz, C. Sicot, L.E. Brizzi, J. Borée, Y. Gervais, "Pressure/velocity coupling induced by a near wall wake", *Exp. Fluids* **49**(1), 147-165 (2010)

[8] C. Hoarau, J. borée, J. laumonier, Y. gervais, "Unsteady wall pressure field of a model A-pillar conical vortex", *Int. J. Heat and Fluid Flow* **29**, 812-819 (2008)

[9] D. Leclercq, "Modelisation de la réponse vibro-acoustique d'une structure couplée à une cavité en presence d'un écoulement turbulent", PhD., Université de Technologie de Compiègne (1999)

[10] M. Kiya, K. Sasaki, "Structure of a turbulent separation bubble", *J Fluid Mech.* **137**, 83-113 (1983)

[11] N.J. Cherry, R. Hillier, M.E.M.P. Latour, "Unsteady measurements in a separated and reattaching flow", *J. Fluid Mech.* **144**, 13-46 (1984)

[12] J.F. Largeau, "Analyse experimentale de la dynamique et du rayonnement acoustique d'un écoulement de marche montante", PhD., Université de Poitiers (2004)

[13] J.S. Bendat, A.G. Piersol, "Random data analysis and measurement procedures", 3rd edition (Wiley, New York) (2000)